Field Quantization and Metrical Geometry on a Simplicial Lattice

Jorge L. deLyra*
Departamento de Física Matemática
Instituto de Física da Universidade de São Paulo
Caixa Postal 66318, 05315–970
São Paulo, SP, Brazil

July 1998

Abstract

We present here the results of stochastic simulations which show that the quantization of the $\lambda\phi^4$ model on a periodical Euclidean lattice in the presence of localized external sources produces a discrete curved metrical geometry on a simplicial complex defined over the lattice. The intrinsic physical scale defined by the correlation length produced by the quantization process plays a central role in the definition of this geometry. The renormalized mass associated to this correlation length is measured on single links and plaquette diagonals of the lattice by means of local observables related to the two-point function.
PACS:03.70.+k;11.10.-z

Submitted to Nuclear Physics.

*E-mail address: delyra@fma.if.usp.br; home page: http://www.fma.if.usp.br/~delyra/

1 Review of the Model

Consider the $SO(2)$-invariant $\lambda\phi^4$ model as defined in the usual way, on a 4-dimensional cubical Euclidean lattice with periodical boundary conditions and N sites in each direction, labeled by integer coordinates $n_\mu = 1, \ldots, N$, $\mu = 1, \ldots, 4$,

$$S_N[\varphi] = \sum_{n_1=1}^{N} \cdots \sum_{n_4=1}^{N} \left[\frac{1}{2} \sum_{\mu=1}^{4} \Delta_\mu \vec{\varphi} \cdot \Delta_\mu \vec{\varphi} + \frac{\alpha}{2} \vec{\varphi} \cdot \vec{\varphi} + \frac{\lambda}{4} (\vec{\varphi} \cdot \vec{\varphi})^2 - \vec{\jmath} \cdot \vec{\varphi} \right], \tag{1}$$

where $\varphi_i(n_1, \ldots, n_4)$, $i = 1, 2$ are the dimensionless field variables, α is the dimensionless mass parameter, λ the dimensionless coupling constant, Δ_μ is the forward difference, the dot denotes scalar product in the internal space of the fields $\vec{\varphi} = (\varphi_1, \varphi_2)$, and $\vec{\jmath} = (j_1, j_2)$ is an external source. The summation convention will not be used here, sums over μ will be written explicitly.

One can take a classical continuum limit of this model. The classical solution on a finite lattice is the configuration of the field $\vec{\varphi}$ that minimizes the function $S_N[\varphi]$, which has a lower bound if $\lambda > 0$ or if $\lambda = 0$ with $\alpha \geq 0$. In order to take the continuum limit, it is necessary that we introduce a dimensional parameter in the system, so that it will be possible to define the concept of distance between points on the lattice. Classically we assume that, in some system of units *external* to the model, our cubic lattice has sides of length L. We define then the lattice spacing as $a = L/N$, the squared mass as $m^2 = \alpha a^{-2}$, the dimensional field as $\vec{\phi} = \vec{\varphi} a^{-1}$ and the dimensional external source as $\vec{J} = \vec{\jmath} a^{-3}$. Taking now the limit $N \to \infty$ with fixed L and $a \to 0$, we have that $S_N[\varphi] \to S[\phi]$ where

$$S[\phi] = \int_V d^4x \left[\frac{1}{2} \sum_{\mu=1}^{4} \partial_\mu \vec{\phi} \cdot \partial_\mu \vec{\phi} + \frac{m^2}{2} \vec{\phi} \cdot \vec{\phi} + \frac{\lambda}{4} \left(\vec{\phi} \cdot \vec{\phi} \right)^2 - \vec{J} \cdot \vec{\phi} \right]. \tag{2}$$

Hence we recover the classical field theory in its usual continuum form, defined inside a cubical periodical box of volume $V = L^4$.

We may use the lattice to define the quantum theory starting from (1) in the way described in [1]. Unlike the classical theory, the quantum theory has an *intrinsic* physical scale given by the correlation length associated to its renormalized mass. In the continuum limit of the quantum theory it is this intrinsic scale which defines all dimensional quantities, and hence there is no need to introduce an external physical scale. For example, in this case we may measure the size of the box in terms of the intrinsic scale by saying that we can fit L correlation lengths end-to-end along a side of the box. In a complete field theory, containing all the particles and interactions which do in fact exist in nature, this is the only way in which we may define the physical length scale, since there is nothing external to such a complete theory. Here we have only a simple incomplete model, but we would like to treat it as a laboratory for these ideas.

We define a version of the quantum theory on each finite lattice and afterwards consider the limit of the sequence of these finite quantum theories as we increase N indefinitely. In each finite lattice we define the quantum theory as a statistical model

with a finite number of degrees of freedom. The observables are defined in the usual way as

$$\langle \mathcal{O} \rangle = \frac{\int [d\varphi] \mathcal{O}[\varphi] e^{-S_N[\varphi]}}{\int [d\varphi] e^{-S_N[\varphi]}},$$

where $[d\varphi] = \prod_{n_1=1}^{N} \ldots \prod_{n_4=1}^{N} \prod_{i=1}^{2} d\varphi_i(n_1, \ldots, n_4)$.

2 Local Observables

We will be paying particular attention to certain observables related to the finite differences along links and plaquette diagonals of the lattice, namely

$$\begin{aligned} \langle (\Delta_\mu \varphi_i')^2 \rangle &= \langle [\varphi_i'(n_\mu + 1) - \varphi_i'(n_\mu)]^2 \rangle, \\ \langle (\Delta_{\mu_1,\mu_2} \varphi_i')^2 \rangle &= \langle [\varphi_i'(n_{\mu_1} + 1, n_{\mu_2} + 1) - \varphi_i'(n_{\mu_1}, n_{\mu_2})]^2 \rangle, \end{aligned}$$

where we define the shifted field variables by $\varphi_i' = \varphi_i - \langle \varphi_i \rangle$. We may write these observables in terms of the momentum-space propagators by means of finite Fourier transformation, obtaining

$$\begin{aligned} \langle (\Delta_\mu \varphi_i')^2 \rangle &= \sum_{k_1=k_m}^{k_M} \ldots \sum_{k_4=k_m}^{k_M} 4 \sin^2 \left(\pi \frac{k_\mu}{N} \right) \langle |\widetilde{\varphi}_i'(k)|^2 \rangle, \\ \langle (\Delta_{\mu_1,\mu_2} \varphi_i')^2 \rangle &= \sum_{k_1=k_m}^{k_M} \ldots \sum_{k_4=k_m}^{k_M} 4 \sin^2 \left(\pi \frac{k_{\mu_1} + k_{\mu_2}}{N} \right) \langle |\widetilde{\varphi}_i'(k)|^2 \rangle, \end{aligned} \tag{3}$$

where the sum over the integer variables k_μ runs over the Fourier modes of the lattice, with $k_M = 1 - k_m = N/2$ for lattices with even N, while $k_M = -k_m = (N-1)/2$ for lattices with odd N. The finite Fourier transforms, with the normalization we use here, are given by

$$\widetilde{\varphi}_i(k) = \frac{1}{N^4} \sum_{k_1=k_m}^{k_M} \ldots \sum_{k_4=k_m}^{k_M} \exp \left(\imath \frac{2\pi}{N} \sum_{\mu=1}^{4} k_\mu n_\mu \right) \varphi_i(n),$$

and their inverses by

$$\varphi_i(n) = \sum_{n_1=1}^{N} \ldots \sum_{n_4=1}^{N} \exp \left(-\imath \frac{2\pi}{N} \sum_{\mu=1}^{4} k_\mu n_\mu \right) \widetilde{\varphi}_i(k).$$

This gives us relations between local observables defined over individual links and plaquette diagonals of the lattice and the renormalized mass parameter α_R which is contained in the two-point function. As it happens, in the $\lambda\phi^4$ model the momentum-space

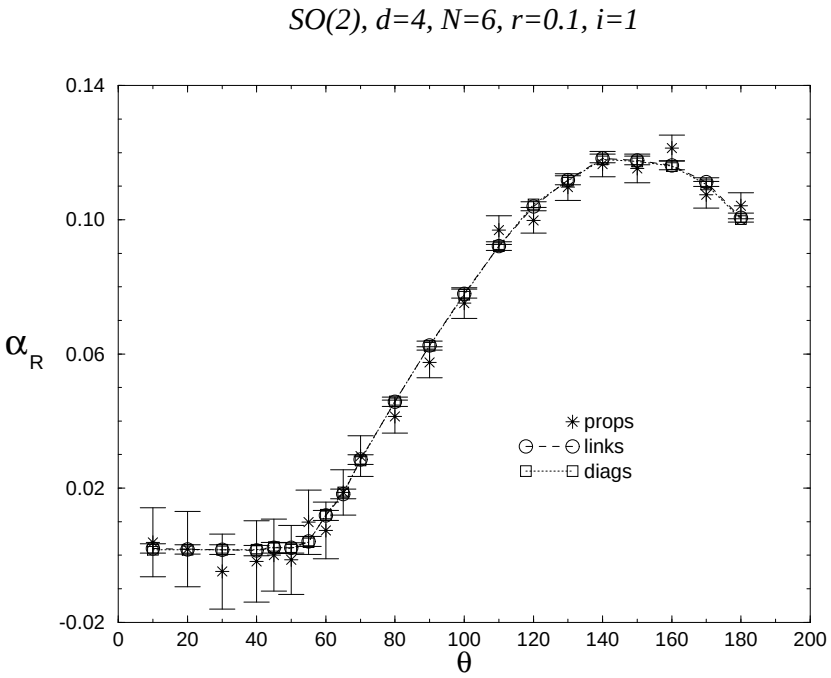

Figure 1: Test of the local observables for field component φ_1 with $N = 6$ and $r = 0.1$.

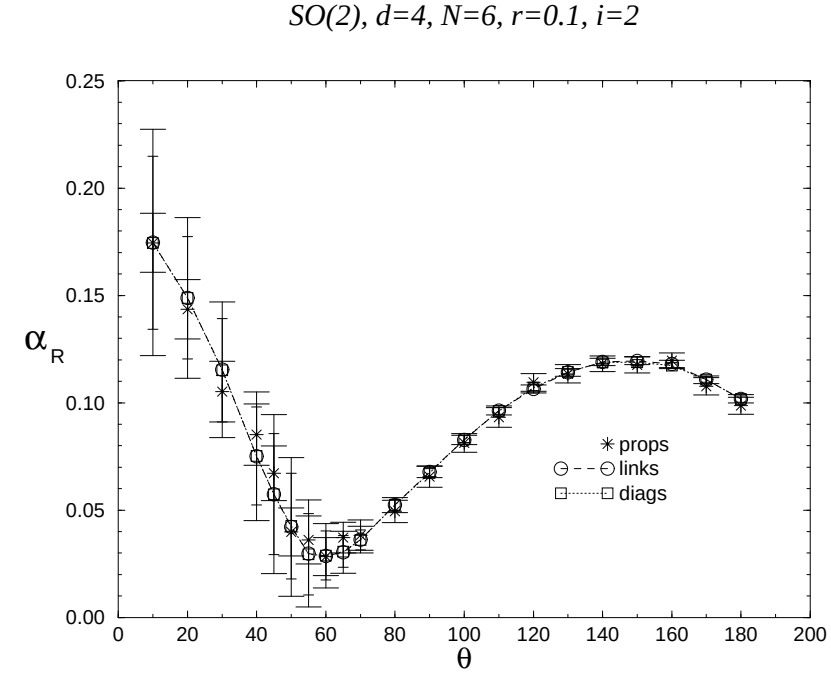

Figure 2: Test of the local observables for field component φ_2 with $N = 6$ and $r = 0.1$.

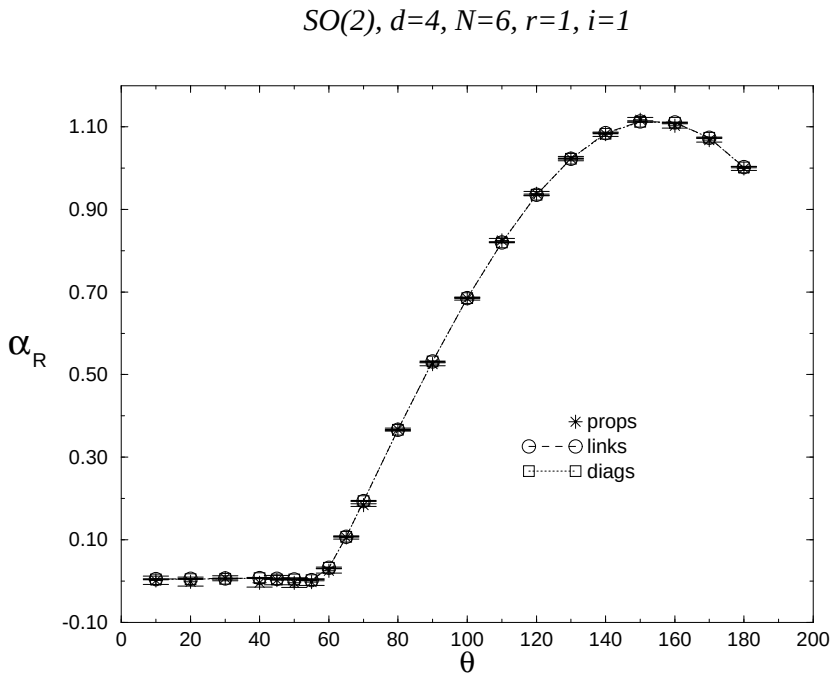

Figure 3: Test of the local observables for field component φ_1 with $N = 6$ and $r = 1.0$.

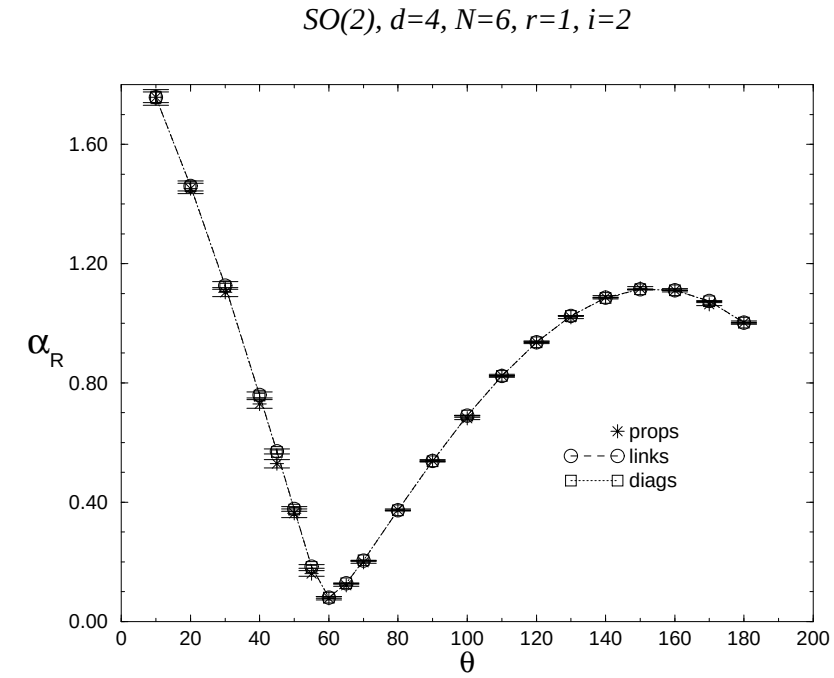

Figure 4: Test of the local observables for field component φ_2 with $N = 6$ and $r = 1.0$.

propagators for each field component can be fitted very precisely by functions of the form

$$\frac{1}{N^4}\,\frac{1}{\rho^2(k)+\alpha_R},$$

for all allowed values of α and λ, in both the symmetric and broken-symmetric phases, where the quantities

$$\rho^2(k) = 4\left[\sin^2\left(\frac{\pi k_1}{N}\right) + \ldots + \sin^2\left(\frac{\pi k_4}{N}\right)\right]$$

are the eigenvalues of the discrete Laplacian. The fact that the propagator of this model does not differ appreciably from the propagator of the free theory has been known for some time. For example, the surprising result reported in Fig. 1 of [2] is equivalent to this. One-loop perturbation theory also gives the same result, which matches very well the non-perturbative predictions of Monte Carlo simulations, as one can see in [1]. If we use this fact, we may write the relations in (3) as

$$\begin{aligned}
\langle(\Delta_\mu\varphi_i')^2\rangle &= \frac{1}{N^4}\sum_{k_1=k_m}^{k_M}\cdots\sum_{k_4=k_m}^{k_M}\frac{4\sin^2\left(\pi\frac{k_\mu}{N}\right)}{\rho^2(k)+\alpha_{R,i}},\\
\langle(\Delta_{\mu_1,\mu_2}\varphi_i')^2\rangle &= \frac{1}{N^4}\sum_{k_1=k_m}^{k_M}\cdots\sum_{k_4=k_m}^{k_M}\frac{4\sin^2\left(\pi\frac{k_{\mu_1}+k_{\mu_2}}{N}\right)}{\rho^2(k)+\alpha_{R,i}}.
\end{aligned} \tag{4}$$

By measuring the left-hand sides and inverting these formulas numerically one is able to obtain the values of the renormalized mass parameters $\alpha_{R,i}$ associated to each field component φ_i. We verified directly, in various situations where the model has discrete translation invariance, that these formulas reproduce very precisely the values of $\alpha_{R,i}$ as obtained directly from their definition as the positions of the poles of the corresponding propagators. These verifications confirm that the propagators of our model can indeed be very well fitted by the form of the propagator of the free theory with appropriate values for its mass parameter. Examples of such verifications can be found in Figs. 1 to 8. The parameters r and θ that appear in these graphs relate to α and λ by

$$\begin{aligned}
\alpha &= -r\cos(\theta),\\
\lambda &= r\sin(\theta).
\end{aligned} \tag{5}$$

In the graphs the results from the fit to the propagator are labeled as props and the two types of results from (4) as links and diags.

3 Lattice Geometry

We see, therefore, that the observables in (4) can be used as a means of measuring $\alpha_{R,i}$. Furthermore, since they are local objects on the lattice, involving only two neighboring

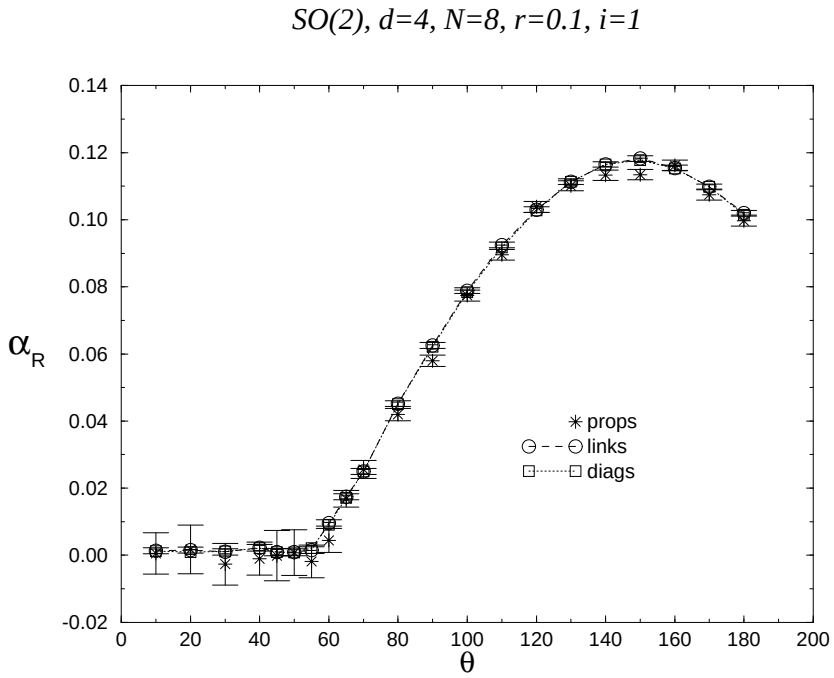

Figure 5: Test of the local observables for field component φ_1 with $N = 8$ and $r = 0.1$.

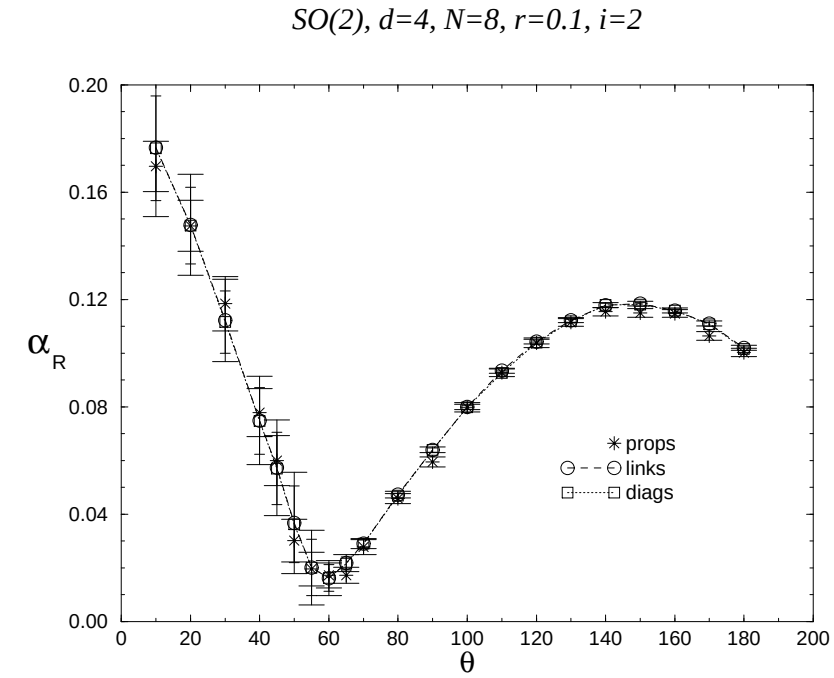

Figure 6: Test of the local observables for field component φ_2 with $N = 8$ and $r = 0.1$.

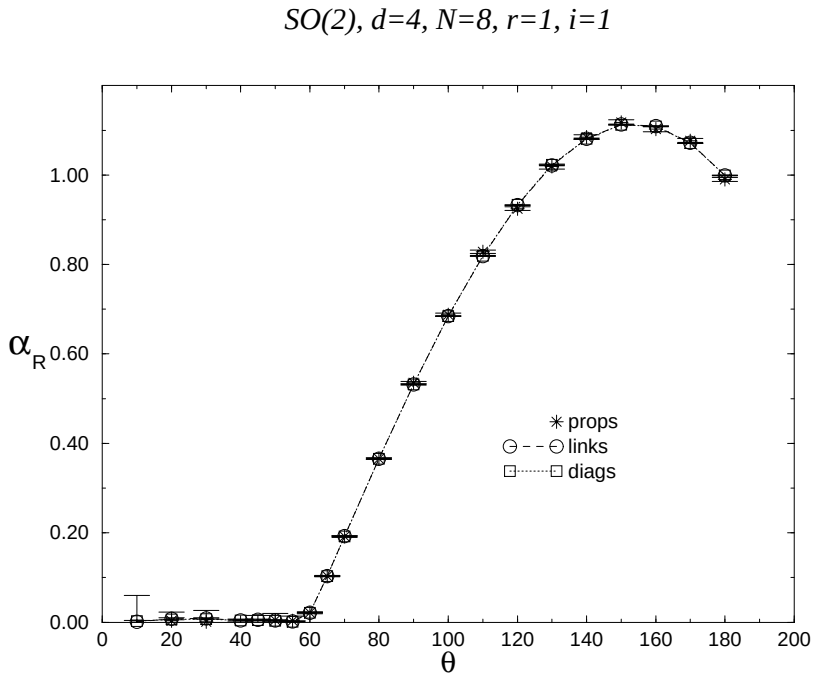

Figure 7: Test of the local observables for field component φ_1 with $N = 8$ and $r = 1.0$.

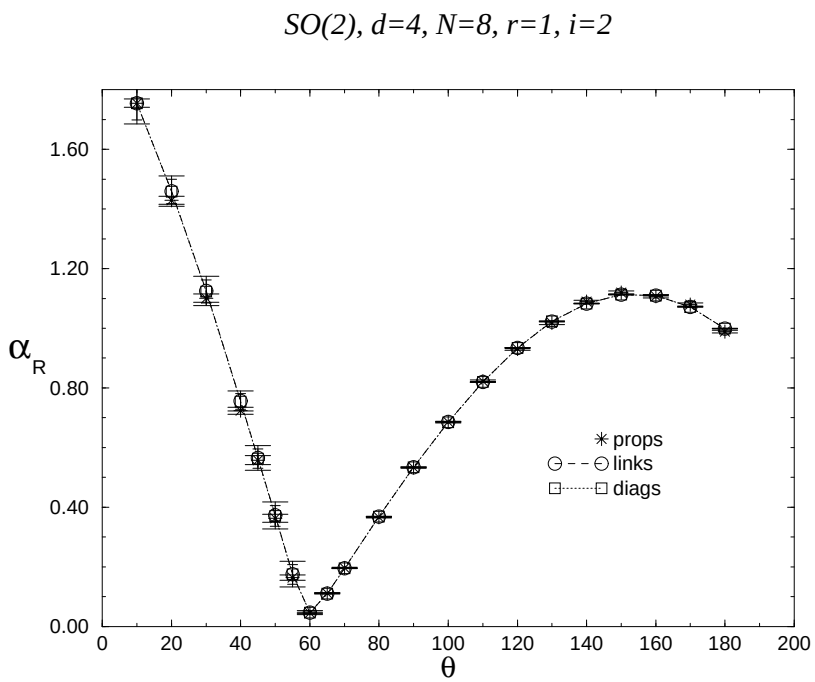

Figure 8: Test of the local observables for field component φ_2 with $N = 8$ and $r = 1.0$.

sites, they allow us to measure $\alpha_{R,i}$ in a *local* way, associating the resulting value to a single link or plaquette diagonal and therefore allowing us to detect dependencies of $\alpha_{R,i}$ on position and direction.

Of course, one does not expect any such dependencies in situations where the discrete translation and rotation invariances of the model are fully realized on the lattice, a fact which is easily verified numerically. However, the introduction of *localized external sources* breaks some of these invariances. External sources are routinely considered in the formalism of the effective action but, in that setting, they are treated as infinitesimal objects and eventually made to vanish. In this paper we consider the effects of non-infinitesimal external sources. These are to be interpreted in the usual way as classical objects interacting with our model, that is, the effects of large agglomerations of energy in bound states such as, for example, classical apparata involved in the production and detection of particles.

With sufficiently strong external sources one observes that, using (4) to measure $\alpha_{R,i}$ for each individual link and plaquette diagonal of the lattice, they indeed depend on position and direction with respect to the location of the source. Using one of the resulting $\alpha_{R,i}$, say for the field component $i = 2$, to define the intrinsic scale of lengths throughout the lattice, and considering that the inclusion of a sufficient number of diagonals of its hyper-cubical cells will turn the lattice into a simplicial complex, one obtains on it a discrete simplicial geometry. Note that here we treat the model as an entity by itself, and insist on using the intrinsic physical scale defined within it to define what is meant by the unit of length. The geometry comes about when we use this intrinsic physical scale to measure the lengths of all links and diagonals of the lattice, and hence of all paths formed by sequences of such elementary geometrical objects.

One can understand the use of relations (4) in a setting where one does not have the usual discrete translation and rotation invariances in the following way. If one has discrete translational invariance, it is clear that the use of finite Fourier transformation is a correct way to extract from the theory the behavior of the two-point function at large distances and hence to determine the renormalized mass. Within this context the equations in (4) establish the relation between the long-range definition of the renormalized mass and the short-range correlations along single links and plaquette diagonals. If one introduces external sources which break discrete translation invariance, then it is no longer so clear how one can extract the renormalized mass from the momentum-space propagator. For example, it is well known that in systems with fixed boundary conditions one must use another set of mode functions for this purpose, which are the eigenfunctions of the Laplacian in those systems [3].

However, the dynamics of the model still implies certain short-range correlations along links and diagonals, although these may no longer be the same for all links or diagonals along the lattice. One may imagine that a link or diagonal of the lattice is also part of a *tangent lattice*, which has the same size and dimension of our lattice but in which there are no external sources and over which the short-range correlations are homogeneous, that is, the same for all the links or diagonals along this tangent lattice. One may think of equations (4) as relating the long-range and short-range correlations

in this tangent lattice. In the continuum limit, the tangent lattice bears to the flat tangent space at each point the same relation that the lattice bears to the (possibly curved) space-time. For sufficiently large lattices any given site will be many links away from the position of the external source and then a small patch of the lattice around the given site can be well approximated by a corresponding portion of the flat tangent lattice.

We imagine that in this tangent lattice there is a set of fields $\varphi_{i(t)}$ similar in type and number to the fields of the actual lattice, with a dynamics given by a similar action. Although on a finite lattice the values of $\langle\varphi_i\rangle$ and $\langle\varphi_i^2\rangle$ will be slightly different for the fields $\varphi_i(+)$ and $\varphi_i(-)$ at each of the two sites on the two ends of any given link or diagonal, the differences disappear in the continuum limit, where the lattice spacing goes to zero and the two sites become infinitely close to one another. Therefore, we may define the tangent lattice as having a homogeneous dynamics producing the average values of $\langle\varphi_i\rangle$ and $\langle\varphi_i^2\rangle$ on both sites. Since in this tangent lattice there is a dynamical system similar to the one in the actual lattice, with two parameters $\alpha_{(t)}$ and $\lambda_{(t)}$, we may adjust these two parameters so that the one-point functions $\langle\varphi_{i(t)}(+)\rangle$ and $\langle\varphi_{i(t)}(-)\rangle$ are both equal to the average of $\langle\varphi_i(+)\rangle$ and $\langle\varphi_i(-)\rangle$ and so that the two-point function in the tangent lattice $\langle\varphi_{i(t)}(+)\varphi_{i(t)}(-)\rangle$ has the same values as $\langle\varphi_i(+)\varphi_i(-)\rangle$ in the actual lattice.

In this fashion we define in a complete way a dynamical system in the tangent lattices at each point of the actual lattice which reproduce locally the observables of the original dynamical system in the actual lattice. This defines the relation between the renormalized mass parameter α_R as defined in the actual lattice and in the tangent lattice, where the dynamics is homogeneous and invariant by discrete translations and rotations and hence where relations (4) hold. The introduction of this tangent structure makes it clear how we may examine the geometry induced by the presence of a non-homogeneous external source even on the rather small lattices which we are able to run with the limited computer resources available. Of course, the simulations will be performed only on the actual lattice, not on the tangent lattices.

4 Results from the Simulations

In order to examine the character of the generated geometry we performed simulations of the model with a constant source located on a single line of sites along the direction $\mu = 1$, which we chose arbitrarily as the temporal direction, representing the world-line of a point source at the origin. In order to obtain the renormalized masses at each link and plaquette diagonal we measured over them the observables defined in (4), for $i = 2$. We used the largest value of the external source along that component that we were able to run, $j_1 = 0$ and $j_2 = 10$. For simplicity of the computational effort we chose to examine the resulting geometry looking at the two-dimensional spatial sections containing the origin, where the source lies. In this way we can examine the geometry through the construction of embeddings of these two-dimensional sections in a fictitious

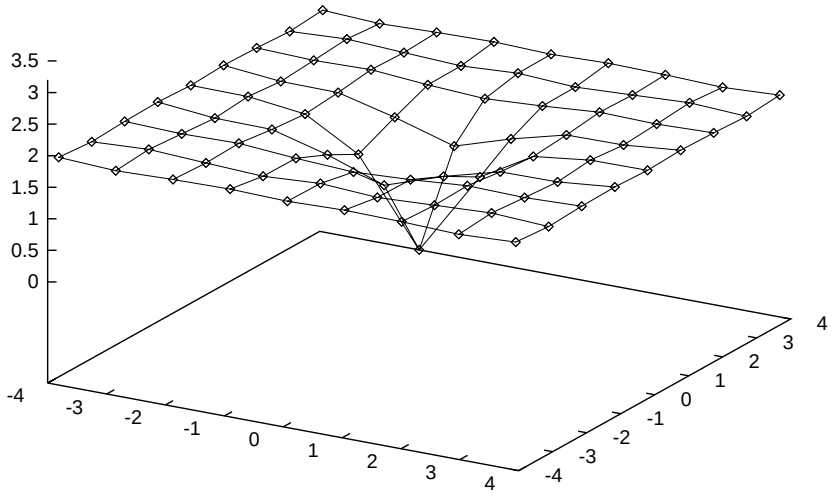

Figure 9: Embedding in the symmetric phase, for $N = 8$, $r = 1$, $\theta = 120^{\rm o}$.

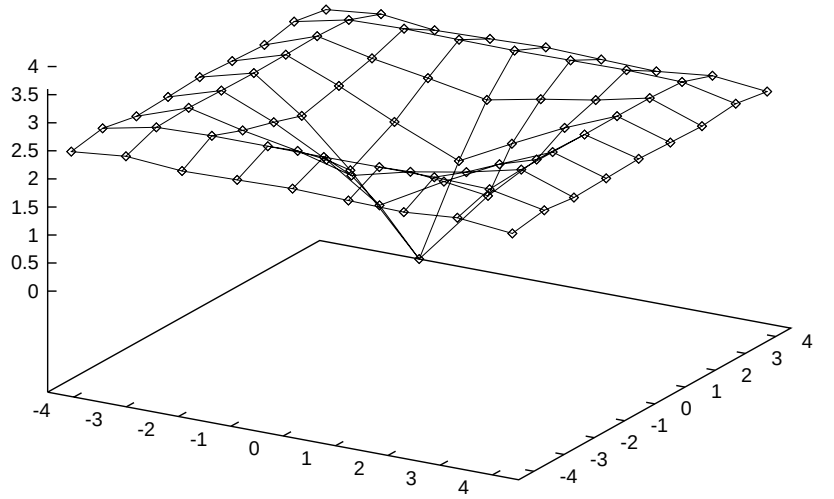

Figure 10: Embedding in the broken-symmetric phase, for $N = 8$, $r = 1$, $\theta = 30^{\rm o}$.

three-dimensional Euclidean space. These sections respect all the translational and rotational symmetries which are left in the system after the introduction of the sources. Due to this, their embeddings should be flat if the four-dimensional intrinsic geometry is flat.

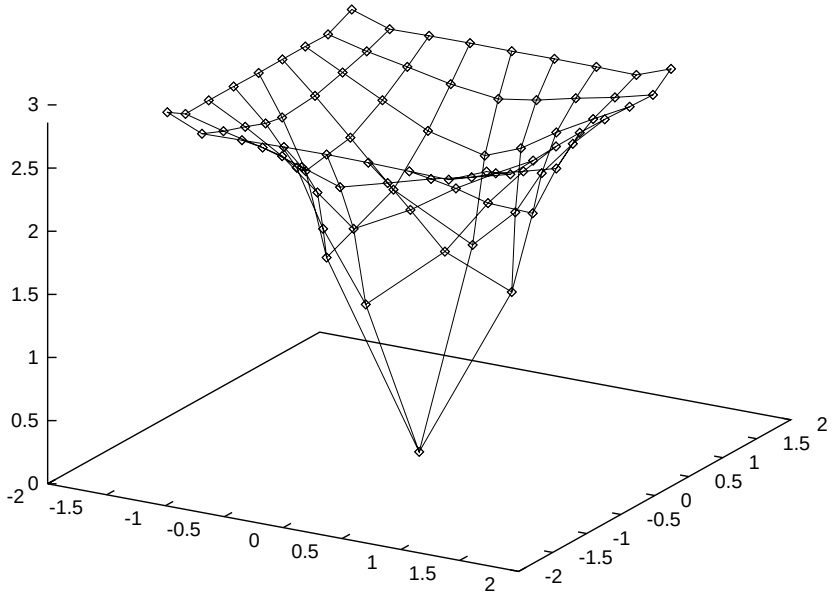

Figure 11: Embedding in the critical region, for $N = 8$, $r = 1$, $\theta = 60^{\rm o}$.

The character of the resulting geometry depends markedly on the location in the (α, λ) parameter plane where the simulations are performed. In the region which becomes the symmetric phase in the continuum limit one obtains a very localized curvature, with a short range around the location of the source, as can be seen in Fig. 9. In the region which becomes the broken-symmetric phase one obtains, quite differently, a geometry with little local curvature but with long range effects and a conical singularity at the position of the source, as can be seen in Fig. 10. In this case a fold in the embedding appears, along the border of the lattice, probably caused by the periodical boundary conditions. The results are particularly interesting in the region close to the continuum-limit critical curve, as can be seen in Fig. 11. In this case one can recognize a clearly curved geometry, particularly so in the vicinity of the source, but extending to the whole lattice.

The scales in these graphs were chosen to give a fair rendition of the embeddings and the overall scale of each graph is not significant, corresponding to a mere change of units of length. The parameters r and θ mentioned in them are those defined in (5). The ranges $\theta \leq 0^{\rm o}$ and $\theta > 180^{\rm o}$ are not allowed, corresponding to the unstable region where λ is negative, and $\theta = 180^{\rm o}$ corresponds to the free theory, in which the geometry

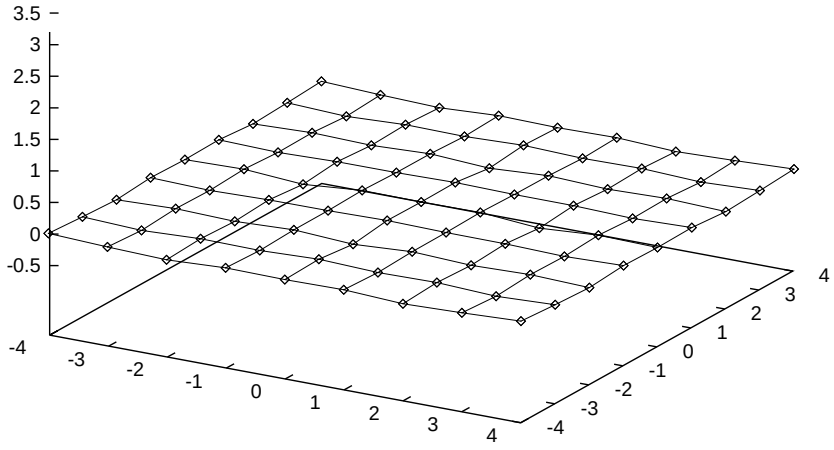

Figure 12: Embedding for the free theory, for $N = 8$, $r = 1$, $\theta = 180^{\circ}$.

should be flat even in the presence of the non-homogeneous external source, as can be easily verified by direct calculation. This case was used to test the programs and it does give a flat geometry, as can be seen in Fig. 12.

For the construction of the embeddings it is necessary to solve an embedding problem which consists of finding a surface in a three-dimensional Euclidean space having the same intrinsic two-dimensional geometry of our section. This problem was solved numerically by a stochastic relaxation process. Note that the embedding problem does not necessarily have a unique solution. There is a drift within the set of possible solutions which happens along with the relaxation process. In order to minimize this drift we perform the relaxation using all the symmetry constraints which we can impose. However, this is not always enough to stabilize completely the embedding, which remains subject to foldings like the one which appears in Fig. 10.

The process of stochastic relaxation was executed in each case until the embedding errors fell below a certain level, chosen to be compatible with our statistical errors. Figs. 13 to 16 contain graphs of the residual embedding errors. The values presented in these graphs correspond to the additional embedding displacements, relative to the average length of the links and diagonals which connect to each site, which it would be necessary to do at each site in order that the errors become zero. Typically the embedding errors are no more than a few percent in the worst cases, in general at the center of the lattice, where the singular source is located, decreasing to negligible levels away from that point. Observe that in general there is no guarantee that there will be

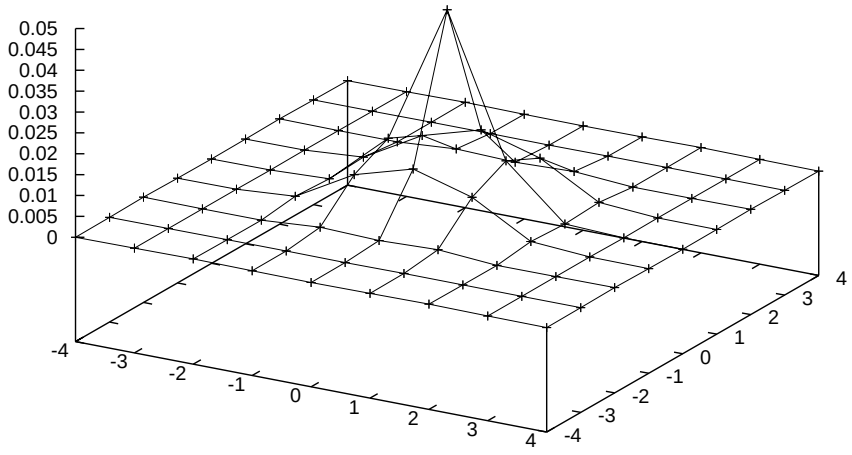

Figure 13: Fractional embedding errors in the symmetric phase, as a function of the integer site coordinates n_μ, for $N = 8$, $r = 1$, $\theta = 120^o$.

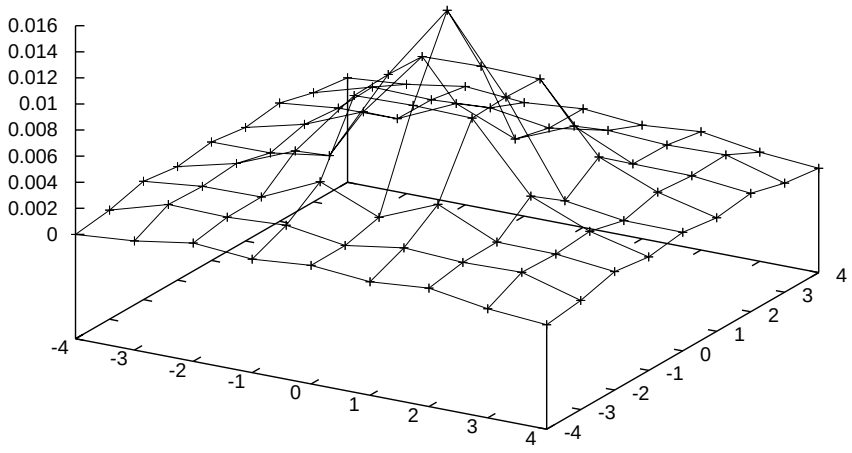

Figure 14: Fractional embedding errors in the broken-symmetric phase, as a function of the integer site coordinates n_μ, for $N = 8$, $r = 1$, $\theta = 30^o$.

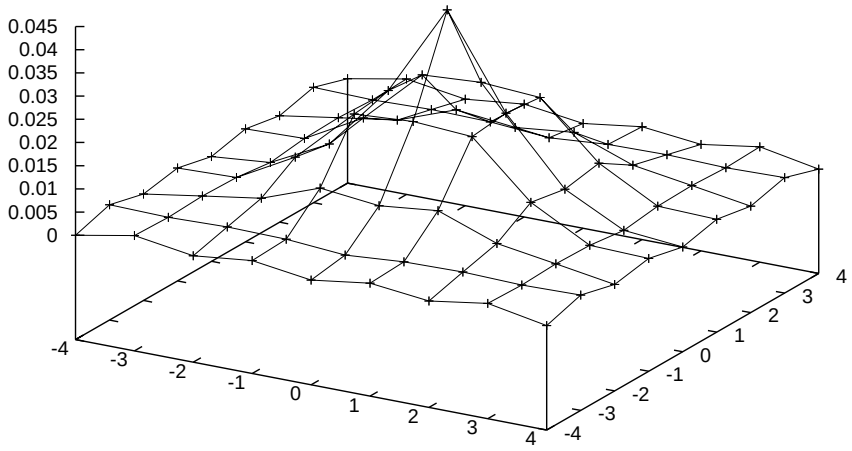

Figure 15: Fractional embedding errors in the critical region, as a function of the integer site coordinates n_μ, for $N = 8$, $r = 1$, $\theta = 60^{\rm o}$.

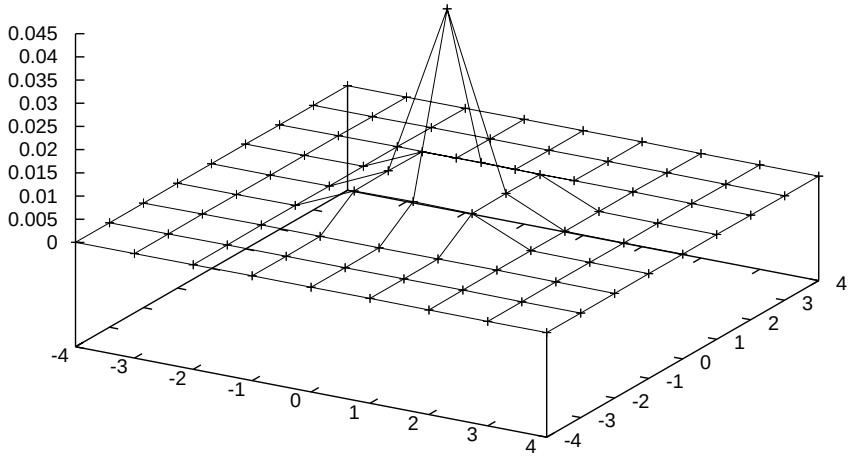

Figure 16: Fractional embedding errors for the free theory, as a function of the integer site coordinates n_μ, for $N = 8$, $r = 1$, $\theta = 180^{\rm o}$.

a solution to the problem of the global embedding of a two-dimensional surface in a three-dimensional Euclidean space. The mere fact that we do find such an embedding with good numerical precision is in itself remarkable, indicating the special character of the generated geometry.

5 Conclusions

We believe that the simulations performed leave little doubt about the fact that the introduction of strong localized external sources in the $\lambda\phi^4$ model generates on the lattice metrical geometries with non-zero intrinsic curvature. We believe that this phenomenon has not been recognized before and that it should be taken into account whenever one considers the definition of quantum-field theoretical models by means of the Euclidean lattice.

Acknowledgements

I would like to thank Prof. Paulo Teotônio Sobrinho for interesting discussions about this work. The computer work involved in this paper was all done on equipment of the University of São Paulo. The major part of the basic simulation work (several thousand hours of CPU time) was done on the IBM-SP2 eight-node parallel computer of the Laboratory for Advanced Scientific Computing (LCCA). The remaining simulation work, as well as all the work of analysis and elaboration of the results, was done on the machines of the Department of Mathematical Physics, with the extensive use of free software, in particular the Debian-GNU-Linux operating system.

References

[1] "Symmetry Breaking on a Finite Euclidean Lattice", J. L. deLyra and A. C. R. Martins, Nucl. Phys. **B432** (1994) 621–640.

[2] "A Monte Carlo Study of ϕ^4 in Four Dimensions", I. A. Fox and I. G. Halliday, Phys. Lett. 159B (1985), 148.

[3] J. L. deLyra, S. K. Foong and T. E. Gallivan, "Finite lattice systems with true critical behavior", Phys. Rev. **D46,** (1992), 1643–1657.